Supplement of Toward hyper-resolution global hydrological models including human activities: application to Kyushu Island, Japan

Naota Hanasaki[1], Hikari Matsuda[1], Masashi Fujiwara[1], Yukiko Hirabayashi[2], Shinta Seto[3], Shinjiro Kanae[4], Taikan Oki[5]

[1]National Institute for Environmental Studies, Tsukuba, Japan
[2]Shibaura Institute of Technology, Tokyo, Japan
[3]Nagasaki University, Nagasaki, Japan
[4]Tokyo Institute of Technology, Tokyo, Japan
[5]University of Tokyo, Tokyo, Japan

Correspondence to: Naota Hanasaki (hanasaki@nies.go.jp)

1 Methods

1.1 Land surface hydrology sub-model localization

The land surface hydrology sub-model resolves the surface energy and water balance. Evapotranspiration (*ET*) is estimated using Equation S1.

$$ET = \beta \rho C_D U (q_{SAT}(T_S) - q_a) \quad \text{(S1)}$$

Here, β is evaporation efficiency, which is a function of effective soil moisture (defined below), ρ is the density of air [kg m^{-3}], C_D is the bulk transfer coefficient, U is the wind speed [m s^{-1}], q_{SAT} is the specific humidity at saturation [kg kg^{-1}], T_S is the surface skin temperature [K], and q_a is the specific humidity [kg kg^{-1}].

The effective soil moisture (W) [kg m^{-2}] is estimated using Equation S2.

$$dW/dt = Rainf + Q_m - ET - Q_s - Q_{sb} - Q_b \quad \text{(S2)}$$

Here, $Rainf$ is rainfall [kg m^{-2} s^{-1}], Q_m is snowmelt [kg m^{-2} s^{-1}], Q_s is surface runoff [kg m^{-2} s^{-1}], Q_{sb} is interflow [kg m^{-2} s^{-1}], and Q_b is baseflow. W ranges from 0 (soil moisture at the wilting point) to W_f (at field capacity). We assume that the water holding capacity between the wilting point and field capacity is $0.15 \cdot SD$, where SD is soil depth [m]. Surface runoff is generated only if the effective soil moisture exceeds W_f.

Interflow is estimated with Equation S3.

$$Q_{sb} = \frac{W_f}{\tau \times 86400} \left(\frac{W}{W_f} \right)^{\gamma} \quad \text{(S3)}$$

Here, τ is the time constant [day], and γ is the shape coefficient. Baseflow follows the same equation as S3, but with the parameters τ, γ and W_f. uniformly fixed at 100 days, 2, and 150 kg m^{-2}, respectively (Hanasaki et al., 2018).

These equations include four hydrological parameters, namely the bulk transfer coefficient (C_D), soil depth (SD), the shape parameter (γ), and the time constant (τ). The default parameter values for global simulation are 0.003, 1.0 m, 2.0, and 100 days, respectively, representing grassland vegetation. For regional simulations, land use and hydrological characteristics are expressed through modification of these parameters. For example, Mateo et al. (2014) found that the simulation performed best with the values of 0.007, 3.5 m, 2.3, and 155 days, respectively, in the Chao Phraya River, Thailand.

To estimate a plausible set of hydrological parameters in the study domain, a systematic parameter sensitivity test was conducted for the calibration period of 2001 to 2006, using the parameters shown in Table S1. Column B shows the default parameter values adopted for the global simulation. We performed a total of 81 simulations using combinations of three possible values for each parameter, and then calculated Nash-Sutcliffe efficiency at gauging stations on nine major rivers. The parameter combination that yielded the highest NSE for each basin is shown in Table S2. The most frequently selected option for each hydrological parameter was B (1.00 m) for *SD*, A (0.002) for C_D, B (2.0) for γ, and A (25 days) for τ.

Table S1 Parameters tested in this study.

	A	B	C
SD	0.25	1.00	4.00
C_D	0.002	0.006	0.010
γ	1.00	2.00	3.00
τ	25	100	400

Table S2 Parameter combination yielding the best performance for river discharge simulation.

River	SD	C_D	γ	τ
Chikugo	B	A	C	A
Oyodo	B	A	B	A
Kuma	B	A	C	A
Gokase	B	A	B	A
Sendai	C	A	A	C
Oono	B	B	A	A
Midori	B	A	B	B
Onga	B	C	B	A
Kikuchi	B	B	A	A
Most frequent	B	A	B	A

1.2 Reservoir operation sub-model localization

As shown in Figure 2, the localized reservoir operation sub-model requires 12 parameters that characterize the release and storage curves. Using long-term daily reservoir operation records and reservoir operation rules disclosed by dam operators, we identified these parameter values, which are listed in Tables S3–S5.

Table S3 Parameters for the release curve. Four points are shown on time-release coordinates. Time and release are shown as Day of Year (DOY) and $m^3 s^{-1}$, respectively.

	R1	R2	R3	R4
Shimouke	152-7.92	152-12.00	274-12.00	274-7.92
Midorikawa	152-14.39	152-20.07	274-20.07	274-14.39
Tsuruda	152-24.56	152-43.10	274-43.10	274-24.56
Ichifusa	152-8.01	152-12.56	274-12.56	274-8.01
Kitagawa	152-7.97	152-11.73	274-11.73	274-7.97
Iwase	152-19.70	152-23.32	274-23.32	274-19.70

Table S4 Parameters for the upper storage curve. Four points are shown on time-storage coordinates. Time and storage are shown as Day of Year (DOY) and percentage of total storage capacity (%), respectively.

	U1	U2	U3	U4
Shimouke	16-100	162-13	202-63	274-100
Midorikawa	16-68	213-50	274-68	274-68
Tsuruda	16-92	162-41	244-72	274-92
Ichifusa	16-62	16-62	16-62	16-62
Kitagawa	16-82	16-82	16-82	16-82
Iwase	16-39	16-39	16-39	16-39

Table S5 Parameters for the lower storage curve. As the lower storage curve was not explicitly shown, dead storage was used for all dams throughout the year.

	L1	L2	L3	L4
Shimouke	365-12	365-12	365-12	365-12
Midorikawa	365-23	365-23	365-23	365-23
Tsuruda	365-20	365-20	365-20	365-20
Ichifusa	365-13	365-13	365-13	365-13
Kitagawa	365-35	365-35	365-35	365-35
Iwase	365-28	365-28	365-28	365-28

2 Data

2.1 Explicit aqueducts

Numerous weirs have been constructed on Kyushu Island, complicating the selection of weirs to include in the simulation. We first identified regions with water insufficiency from the Water Sustainability Index map. Then, we intensively surveyed the irrigation and municipal water supply systems in those regions and eventually identified six weirs that must be explicitly incorporated into the model (Table S6). Finally, we georeferenced the weirs onto the digital river network, and created the origin and destination relationships among grid cells (Figure S1).

Table S6 Explicit aqueducts implemented in this study.

Weir	River	Location
Shiroishi Zeki	Kikuchi River	E130.575 N32.942
Chikugo Ozeki	Chikugo River	E130.475 N33.325
Water treatment plant of Oita City	Ono River	E131.692 N33.242
Water treatment plant of Oita City	Oita River	E131.608 N33.208
Water treatment plant of Usa City	Yakkan River	E131.342 N33.558
Kawakami Toshuko	Kasegawa River	E130.275 N33.308

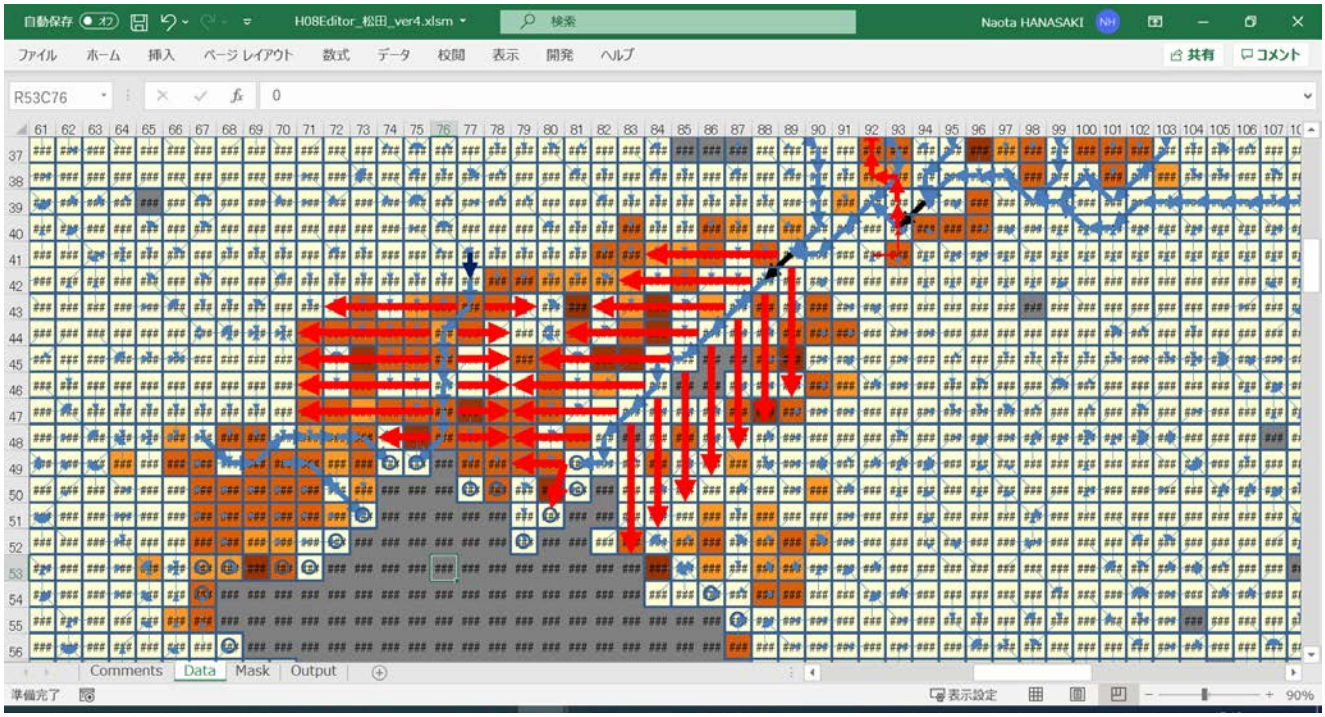

Figure S1 Screenshot of the explicit aqueduct editor in Microsoft Excel. Blue arrows are flow directions. Bold arrows indicate major rivers. Thick black arrows indicate major weirs. Red arrows are explicit aqueducts. The origins of explicit aqueducts are expanded downstream of weirs to avoid possible sudden and unrealistic variations in water abstraction in weir-containing grid cells. The base map shows the Water Sustainability Index, with red indicating water scarcity based on the H08 model with the original implicit aqueduct algorithm (LOC-I1 in Figure 8).

3 Results

3.1 Discharge

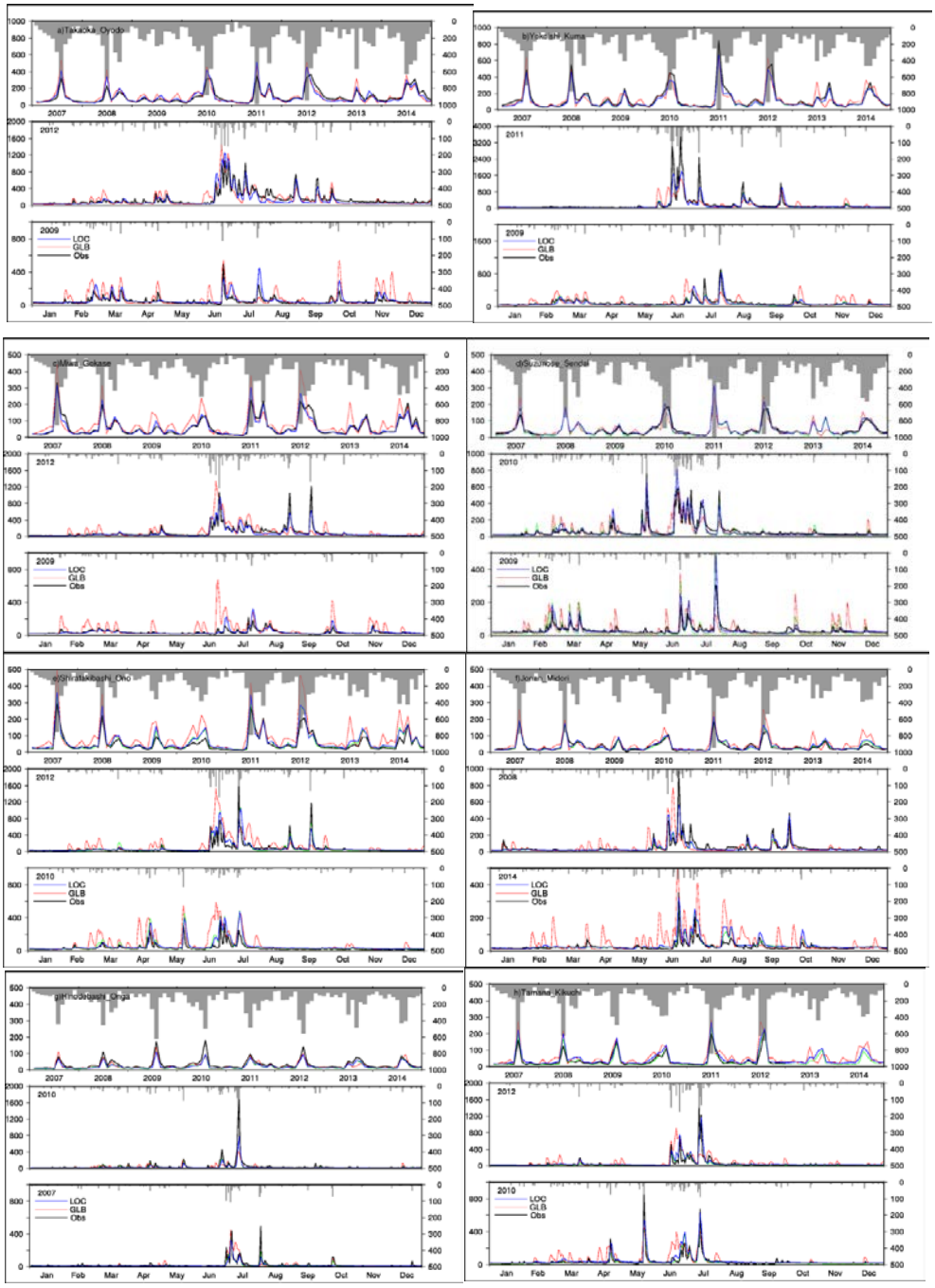

Figure S2 River discharge at a) Takaoka on the Oyodo River, b) Yokoishi on the Kuma River, c) Miwa on the Gokase River, d) Suzunose on the Sendai River, e) Shiratakibashi on the Oono River, f) Jonan on the Midori River, g) Hinodebashi on the Onga River, and h) Tamana on the Kikuchi River. Top: monthly time series of streamflow (lines) and basin-averaged precipitation (bars). Middle: daily time series of streamflow and precipitation in the wettest year of the validation period. Bottom: daily time series of streamflow and precipitation in the driest year of the validation period.

3.2 Irrigation

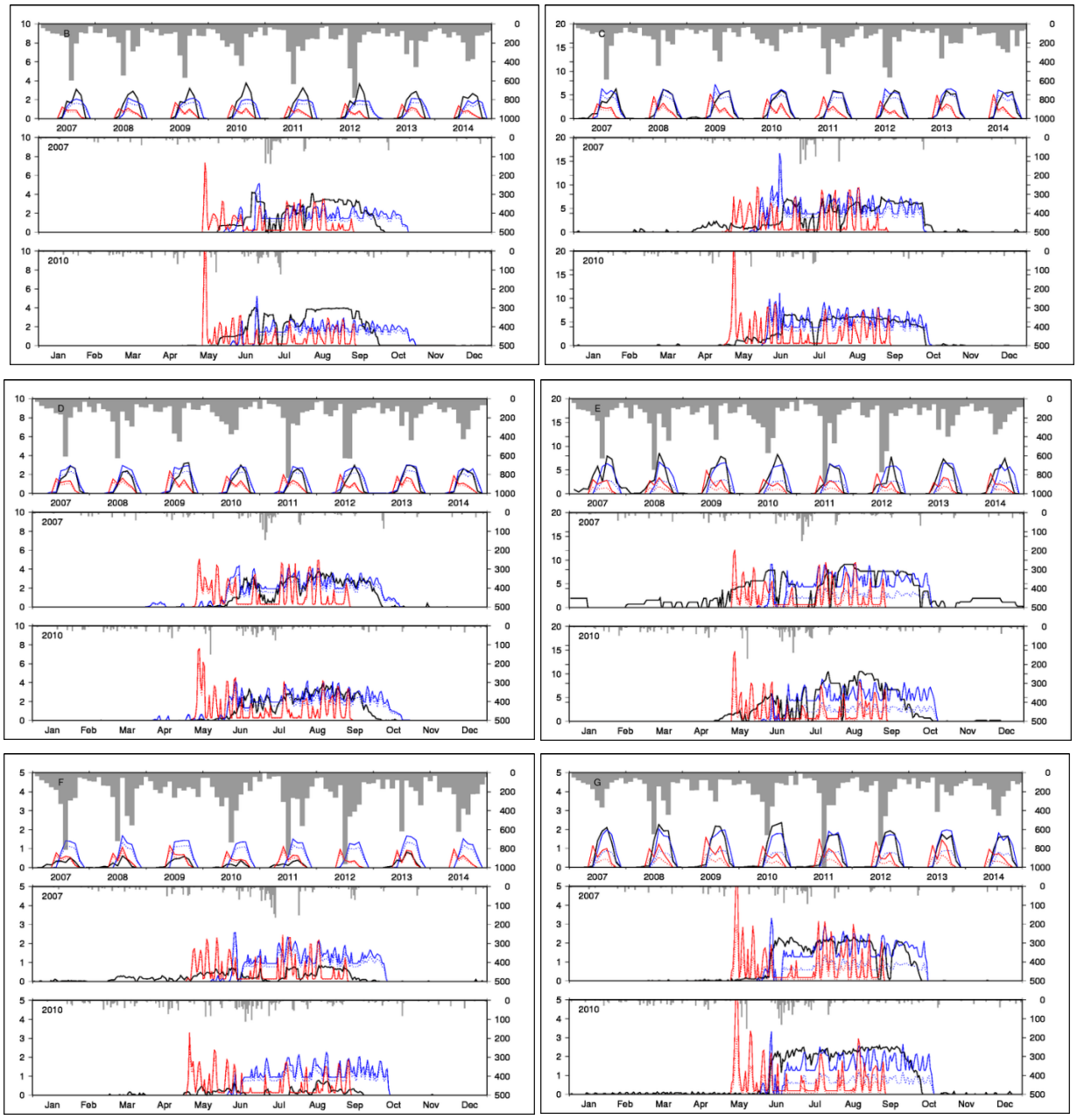

Figure S3 Irrigation water requirement at irrigation projects B–G. Top: monthly time series of irrigation water withdrawal (lines) and basin-averaged precipitation in the LOC simulation (bars). Blue and red lines represent the LOC and GLB simulations, respectively. Solid and broken lines indicate simulations including and excluding irrigation efficiency, respectively. Middle: daily time series of irrigation water and precipitation in the wettest year of the validation period. Bottom: daily time series of irrigation water and precipitation in the driest year of the validation period.

3.3 Dam operation

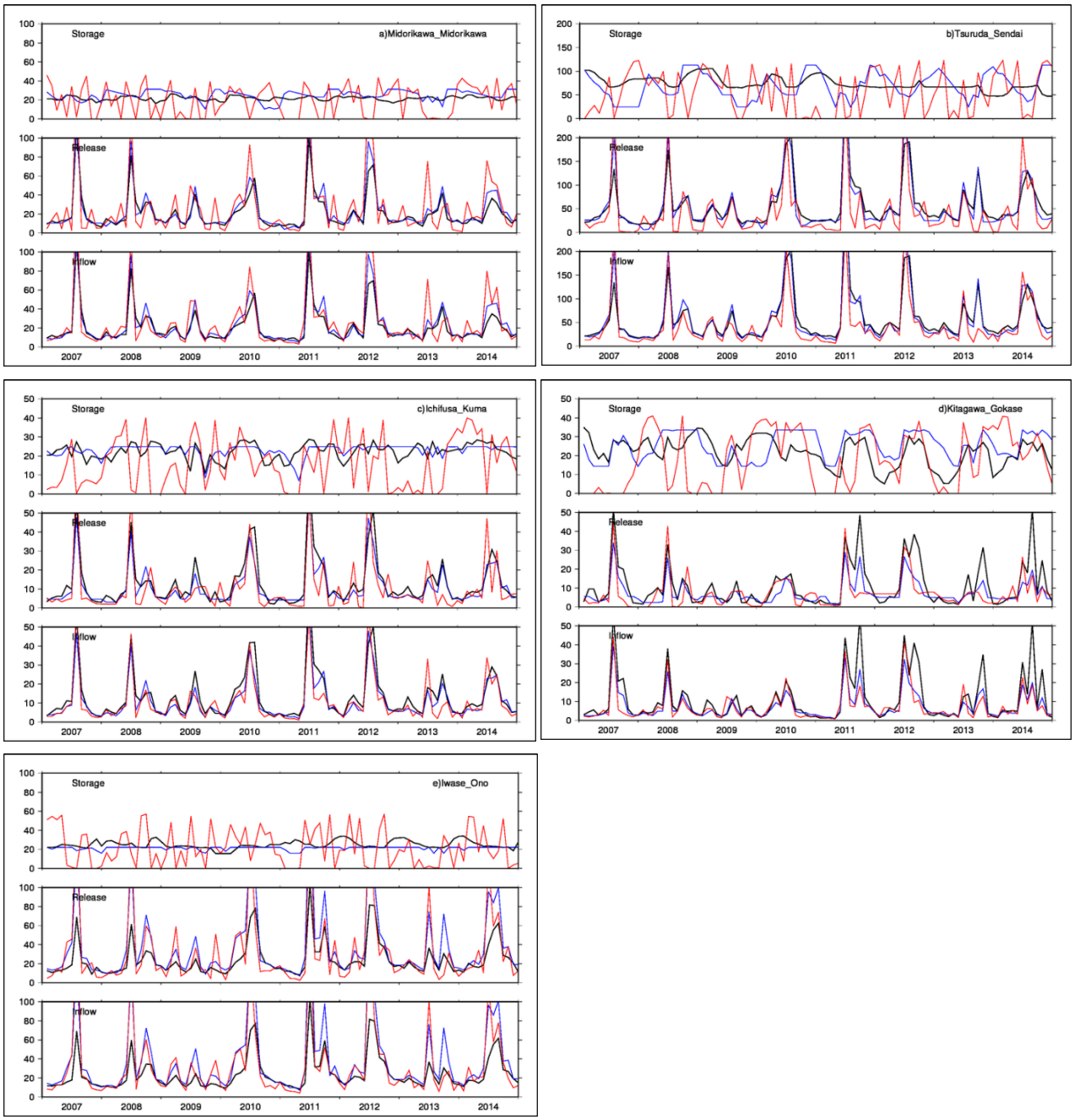

Figure S4 Reservoir operations at a) Midorikawa Dam, b) Tsuruda Dam, c) Ichifusa Dam, d) Gokase Dam, and e) Iwase Dam. Top: monthly time series of water storage (10^6 m^3 $year^{-1}$). Middle: monthly time series of release (m^3 $year^{-1}$). Bottom: monthly time series of inflow (m^3 $year^{-1}$). Blue, red, and black lines indicate the LOC and GLB simulations and observations, respectively.

3.4 Locations with low WSI

105

Figure S5 The locations with low WSI. The background is an enlarged view of Figure 8 (d).

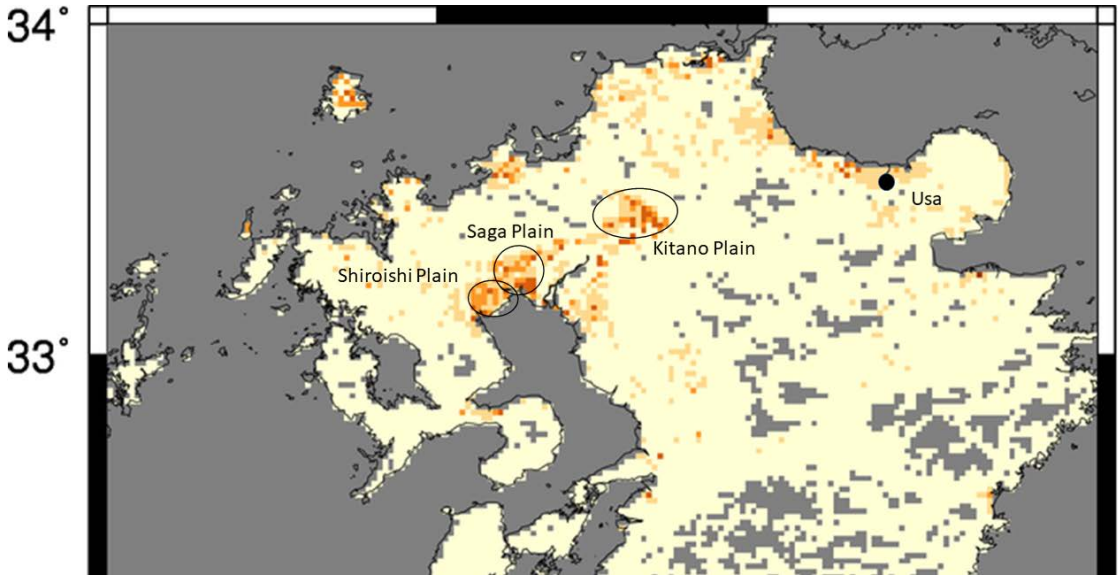

Table S7 Selected information sources for the five assessed regions

Region	Item		Source
Saga Plain	History		https://suido-ishizue.jp/kokuei/kyushu/F1/F2/0101.html
	Kasegawa River		http://www.qsr.mlit.go.jp/takeo/kasegawa/
	Hokuzan (22.5 10^6 m^3)	Dam	http://damnet.or.jp/cgi-bin/binranA/All.cgi?db4=2524
Shiroishi Plain	Water management		https://www.maff.go.jp/kyusyu/nn/new/08/pdffile/saihyouka.pdf
	Groundwater use		http://www.env.go.jp/water/jiban/directory/41saga/chikugo/index.html
Ryochiku Plain	History		https://suido-ishizue.jp/kokuei/kyushu/Prefectures/4002/4002.html
	Chikugogawa River		https://www.mlit.go.jp/common/000230578.pdf
	Egawa	Dam	http://damnet.or.jp/cgi-bin/binranA/

	(25.3 10^6 m^3)		All.cgi?db4=2424
	Terauchi	Dam	http://damnet.or.jp/cgi-bin/binranA/
	(18.0 10^6 m^3)		All.cgi?db4=2430
	Water management		https://www.water.go.jp/chikugo/
			ryochiku/pdf/h27_outline.pdf
Usa	History		https://suido-
			ishizue.jp/kokuei/kyushu/oita/yakkangawa/0101.html
	Hisashi	dam	http://damnet.or.jp/cgi-bin/binranA/
	(4.8 10^6 m^3)		All.cgi?db4=2764
	Hiju	dam	http://damnet.or.jp/cgi-bin/binranA/
	(8.0 10^6 m^3)		All.cgi?db4=2763

References

Hanasaki, N., Yoshikawa, S., Pokhrel, Y., and Kanae, S.: A global hydrological simulation to specify the sources of water used by humans, Hydrol. Earth Syst. Sci., 22, 789-817, 10.5194/hess-22-789-2018, 2018.

Mateo, C. M., Hanasaki, N., Komori, D., Tanaka, K., Kiguchi, M., Champathong, A., Sukhapunnaphan, T., Yamazaki, D., and Oki, T.: Assessing the impacts of reservoir operation to floodplain inundation by combining hydrological, reservoir management, and hydrodynamic models, Water Resources Research, 50, 7245-7266, 10.1002/2013wr014845, 2014.